Chinese Journal of Natural Medicines

Discovery and bioassay of disubstituted β-elemene-NO donor conjugates: synergistic enhancement in the treatment of leukemia

Junlong ZHU, Xiaoying JIANG, Xinyu LUO, Yuan GAO, Rui ZHAO, Junjie LI, Hong CAI, Xiawen DANG, Xiangyang YE, Renren BAI, Tian XIE

Citation: Junlong ZHU, Xiaoying JIANG, Xinyu LUO, Yuan GAO, Rui ZHAO, Junjie LI, Hong CAI, Xiawen DANG, Xiangyang YE, Renren BAI, Tian XIE, Discovery and bioassay of disubstituted β-elemene-NO donor conjugates: synergistic enhancement in the treatment of leukemia, Chinese Journal of Natural Medicines, 2023, 21(12), 916-926. doi: 10.1016/S1875-5364(23)60404-2.

View online: https://doi.org/10.1016/S1875-5364(23)60404-2

Available online at www.sciencedirect.com
ScienceDirect
Chinese Journal of Natural Medicines 2023, **21**(12): 916-926
doi: 10.1016/S1875-5364(23)60404-2
Chinese Journal of Natural Medicines

•Original article•

Discovery and bioassay of disubstituted *β*-elemene-NO donor conjugates: synergistic enhancement in the treatment of leukemia

ZHU Junlong[1, 2Δ], JIANG Xiaoying[1, 2Δ], LUO Xinyu[1, 2], GAO Yuan[1, 2], ZHAO Rui[1, 2], LI Junjie[1, 2], CAI Hong[1, 2], DANG Xiawen[1, 2], YE Xiangyang[1, 2*], BAI Renren[1, 2*], XIE Tian[1, 2*]

[1] *School of Pharmacy, Hangzhou Normal University, Hangzhou 311121, China;*
[2] *Key Laboratory of Elemene Class Anti-cancer Chinese Medicines; Engineering Laboratory of Development and Application of Traditional Chinese Medicines; Collaborative Innovation Center of Traditional Chinese Medicines of Zhejiang Province, Hangzhou Normal University, Hangzhou 311121, China*

Available online 20 Dec., 2023

[ABSTRACT] Natural products are essential sources of antitumor drugs. One such molecule, *β*-elemene, is a potent antitumor compound extracted from *Curcuma wenyujin*. In the present investigation, a series of novel 13,14-disubstituted nitric oxide (NO)-donor *β*-elemene derivatives were designed, with *β*-elemene as the foundational compound, and subsequently synthesized to evaluate their therapeutic potential against leukemia. Notably, the derivative labeled as compound **13d** demonstrated a potent anti-proliferative activity against the K562 cell line, with a high NO release. *In vivo* studies indicated that compound **13d** could effectively inhibit tumor growth, exhibiting no discernible toxic manifestations. Specifically, a significant tumor growth inhibition rate of 62.9% was observed in the K562 xenograft tumor mouse model. The accumulated data propound the potential therapeutic application of compound **13d** in the management of leukemia.

[KEY WORDS] Antitumor activity; Chronic myeloid leukemia; *β*-elemene; Nitric oxide donor; Structural modification
[CLC Number] R284.2 **[Document code]** A **[Article ID]** 2095-6975(2023)12-0916-11

Introduction

Chronic myeloid leukemia (CML) is a malignant disease characterized by the abnormal proliferation of hematopoietic stem cells. Present clinical modalities for CML management remain limited in their strategies [1]. Allogeneic hematopoietic stem cell transplantation (allo-HSCT) remains a choice for some, whereas others resort to chemotherapy, often accompanied by notable adverse effects and suboptimal therapeutic outcomes [2, 3]. In this context, natural products have emerged over recent decades as a reservoir of therapeutic agents, manifesting significant antitumor efficacies, combined with an advantageous profile of efficiency, minimized toxicity, and commendable safety. Therefore, the exploration and utilization of compounds derived from natural products stand out as a promising strategy for CML intervention [4].

Endowed by the intricacies of natural evolution and the sustained maturation of medicinal herbs, natural products exhibit a diverse spectrum of bioactivities, including anti-inflammatory, antitumor, and anti-depression properties [5, 6]. Consequently, they have ascended as paramount sources for novel drug development over the past decades [7-10]. A testament to this trend is the derivation of numerous antitumor agents from natural products and their analogs, exemplified by the drug elemene [11, 12].

Elemene, a sesquiterpene essential oil, is extracted from the desiccated stem of *Curcuma wenyujin* [12]. Various configurations of elemene have been identified to date, of which *β*-elemene is the main component contributing to the antitumor activity (Fig. 1) [13, 14]. The National Medical Products Administration has granted approvals for both injectable and oral formulsions of elemene [15], recognizing their expansive antitumoral spectrum, making them viable for managing advanced neoplastic conditions. However, the therapeutic utility of elemene is tempered by its pronounced lipophilicity

[Received on] 19-May-2023
[Research funding] This project was supported by the Natural Science Foundation of Zhejiang province (No. LY20H300004), the National Natural Science Foundation of China (Nos. 82073686, 81730108, and 81973635), Scientific Research Foundation for Scholars of HZNU (Nos. 2021QDL026 and 2019QDL003), the Ministry of Science and Technology of China (High-end foreign experts program, Nos. G20200217005 and G2021017004).
[*]**Corresponding author]** E-mails: xyye@hznu.edu.cn; renrenbai@126.com; xbs@hznu.edu.cn
[Δ]These authors contributed equally to this work.
These authors have no conflict of interest to declare.

Fig. 1 ***Curcuma wenyujin*, elemene, and chemical structures of elemene isomers.**

and consequent solubility challenges [16]. Therefore, it is imperative to modify the structural architecture of *β*-elemene and to integrate additional antitumor pharmacophores, aiming to optimize its physicochemical attributes while increasing its antitumor activity.

As a gaseous signaling molecule, nitric oxide (NO) demonstrates a plethora of bioactivities *in vivo* [17, 18]. When generated by cytotoxic macrophages, NO can block DNA synthesis, rendering notable antineoplastic activities against tumor cells [19]. However, the utility of NO is constrained by its intrinsic limitations—rapid diffusion and fleeting half-life—which impede its selective retention and accumulation within specific organ systems. Such challenges necessitate the conjugation of NO donors with other pharmacophores during drug synthesis [20]. Furoxans, classified as mercapto-dependent heterocyclic NO donors, stand out in this context. They operate through their corresponding mercaptan moieties, which facilitate the *in vivo* release of NO, manifesting potent antitumor effects. These donors are characterized by efficient NO release, favorable metabolic degradation profiles, and minimized adverse effects. The structural simplicity of furoxan NO donors enhances their amenability to conjugation with other molecular entities, aiding in the solubilization of lipophilic pharmacophores [21, 22]. More importantly, post-administration, NO donor drugs undergo rapid metabolic processing, culminating in the systemic release of NO, which accentuates their antitumor potential [23]. Such a mechanism presents a promising avenue for leukemia therapeutics [24, 25].

On the molecular design front, the concomitant incorporation of nitrogenous moieties at positions 13 and 14 of *β*-elemene can significantly improve the water solubility and increase its anti-proliferation efficacy [4]. Such strategic molecular modifications potentially harmonize to evoke a synergistic antineoplastic response.

Results and Discussion

Design of β-elemene NO derivatives

The molecular weight of *β*-elemene is only 204, which is far less than 500 for drug-like molecules. This modest weight presents an opportunity, making the conjugation with antitumoral pharmacophores an appealing and feasible avenue for structural enhancement aimed at elevating both its physicochemical attributes and antineoplastic potential. Historically, derivatization endeavors pertaining to *β*-elemene have primarily targeted the position 13, largely driven by the ease of synthesizing the 13-chloro-*β*-elemene intermediate. Concurrent modifications at positions 13 and 14 have been relatively uncharted territories in the realm of *β*-elemene derivatization [26]. Comparative studies have elucidated that while 13-chloro-*β*-elemene and 13,14-dichloro-*β*-elemene present comparable antitumor efficacies, the di-chlorinated variant presents a heightened polarity, facilitating its purification [27].

Based on previous studies, the incorporation of nitrogenous moieties emerges as a promising tactic to potentiate the antitumor activity of *β*-elemene, with piperazine and 3-diazabicyclo [3.3.0] octane demonstrating notable efficacy. In addition, nitrogenous *β*-elemene derivatives can be adeptly tethered to NO donors *via* amide bonds. The ensuing metabolites released from such conjugates are anticipated to manifest robust *in vivo* antineoplastic actions. Taking cue from this premise, 13,14-dichloro-*β*-elemene served as the foundational substrate, onto which nitrogenous heterocycles were grafted through substitution reactions. This yielded derivatives with significantly improved water solubility and antineoplastic potency. Subsequent derivatization efforts led to the design of 13,14-bis-NO-donor-*β*-elemene derivatives by bridging 13,14-diamine-*β*-elemene derivatives with two NO donors (Fig. 2). Upon systemic introduction, these novel derivatives could release high levels of NO, resulting in an apoptosis-promoting effect against tumor cells in the blood. Post NO-release, the nitrogenous *β*-elemene metabolites persist in exerting pronounced antitumor effects.

Chemistry

The synthetic routes for the *β*-elemene intermediates **5** and **6** are outlined in Scheme 1. The chlorination of *β*-elemene (**1**) with NaClO produced the chlorinated intermediate **2**. This compound (**2**) was then subjected to a bis-substitution reaction using either piperazine or 3-diazabicyclo [3.3.0]octane. The reaction cascade afforded intermediates **3** and **4**. A subsequent deprotection step furnished the pivotal

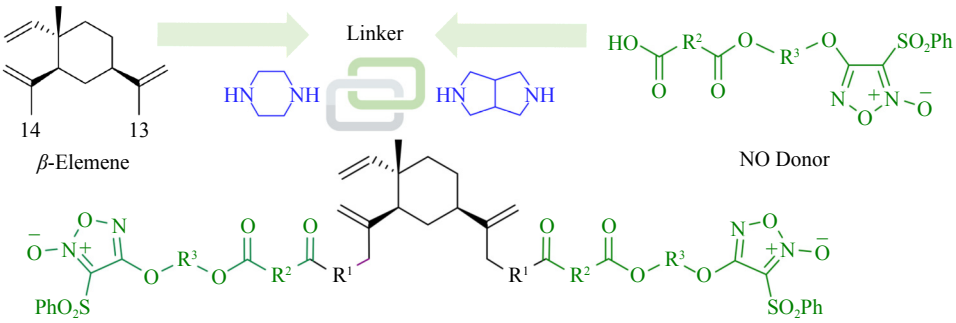

Fig. 2 Design strategy of 13,14-bis-NO donor-*β*-elemene derivatives.

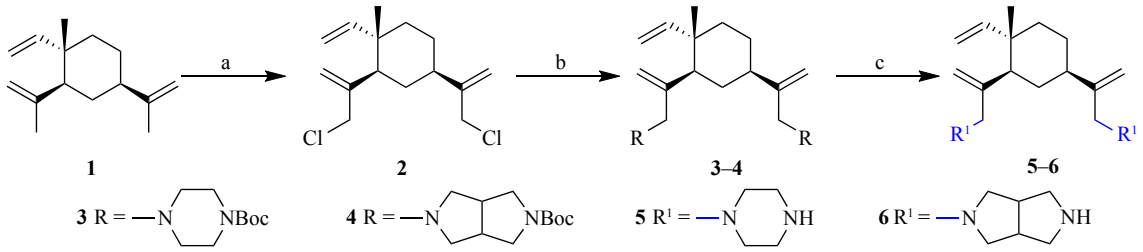

Scheme 1 Synthetic route of intermediates 5−6: (a) NaClO, TBAF, HOAc, and DCM, 0 °C, 5–6 h, 25%; (b) Cs_2CO_3 and DMF, 60 °C, 12 h, 58%–68%; (c) HCl-dioxane and MeOH, 0 °C, 12 h, 95%–97%.

intermediates **5** and **6**.

The NO donor intermediates **9a−b**, **10a−b**, and **11a−b** were prepared as previously described (Scheme 2) [27]. The synthesis procedure began with the sulfonation of phenylmercaptoacetic acid using 30% hydrogen peroxide. Fuming nitric acid treatment in a closed loop produced the key intermediate **8**. This compound reacted with diol under alkaline conditions, followed by esterification with anhydride under DMAP and EDCI treatment, culminating in the synthesis of NO donor intermediates **9a−b**, **10a−b,** and **11a−b**.

As shown in Scheme 3, the final 13,14-bis-NO donor-*β*-elemene derivatives **12a−f** and **13a−f** were synthesized by the amidation reaction of *β*-elemene intermediates **5–6** with the NO donor intermediates **9a−b**, **10a−b**, and **11a−b** under HOBt, EDCI, and DIPEA treatment, respectively.

In vitro efficacy test

In vitro NO release test

To ascertain the potential for stable *in vivo* nitric oxide

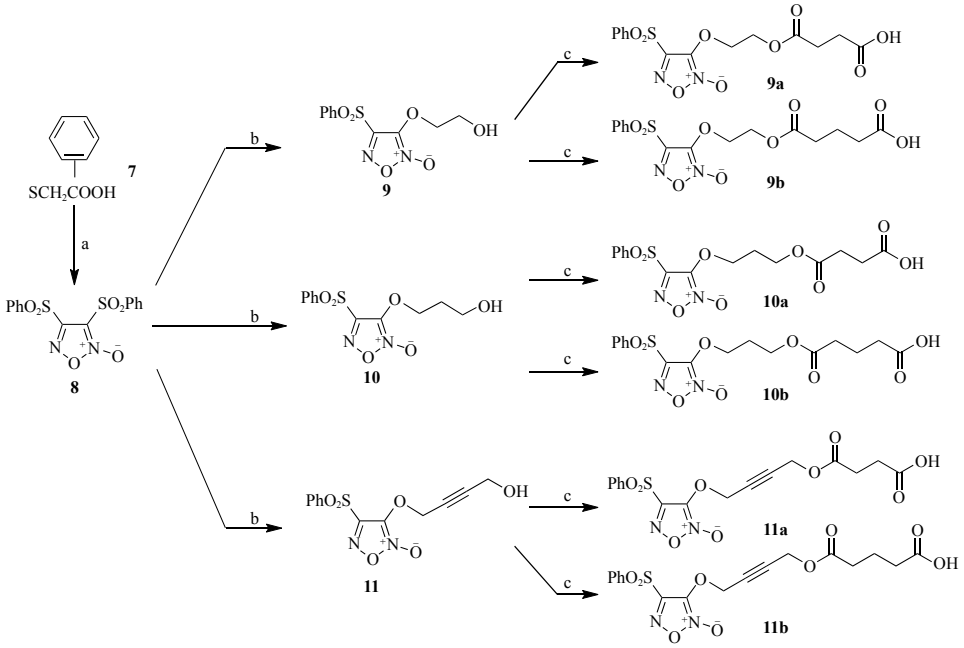

Scheme 2 Synthetic routes of intermediates 9−11: (a-1) 30% H_2O_2 and HOAc, r.t., 5–6 h; (a-2) fuming HNO_3 and HOAc, 140 °C, 2 h, 15%–30%; (b) 15% NaOH, THF, r.t., 2 h, 59%–77%; (c) DMAP and DCM, r.t., 12 h, 60%–90%.

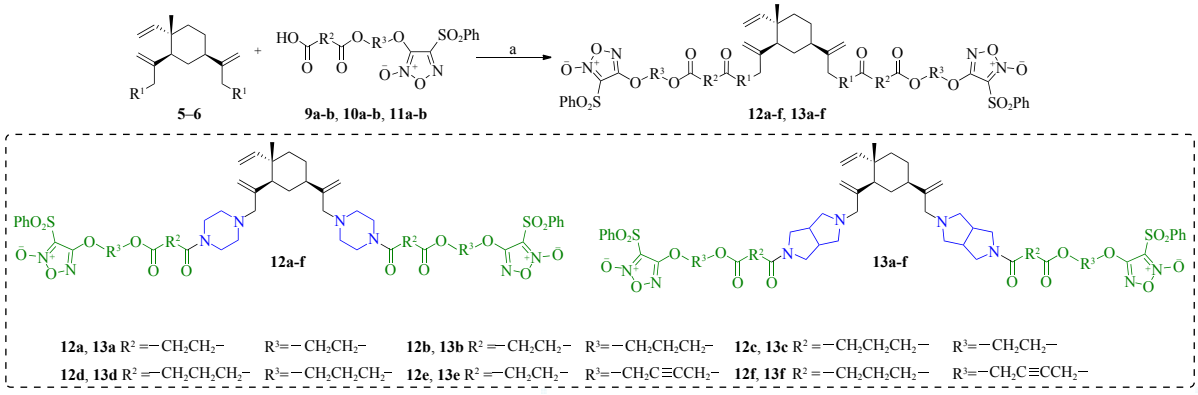

Scheme 3 Synthetic route of compounds 12−13: (a) DIPEA, HOBt, EDCI, and DCM, r.t., 26%−71%.

(NO) release, we conducted *in vitro* tests on the designed compounds. As shown in Table 1, all compounds demonstrated the ability to release NO in the test range. Intriguingly, a consistent augmentation in NO concentration was observed as the duration of the test progressed. Notably, compounds **12a**, **13a**, **13b**, **13d**, **13e,** and **13f** could release high levels of NO efficiently. Diol and anhydride linkers displayed specific effects on the release of NO. Compounds tethered with propylene glycol as a linker demonstrated superior NO release to their counterparts linked with ethylene glycol and 1,4-butynediol. Similarly, those employing glutaric anhydride as a linker yielded higher NO concentrations than compounds conjugated with butanedioic anhydride.

Anti-proliferative evaluation

Initially, all synthesized compounds was subjected to cytotoxicity assays against cell lines K562 (human chronic myeloid leukemia cells), CCRF-CEM (human acute lymphoblastic leukemia T lymphocytes), A375 (human malignant melanoma cells), and SK-MEL-2 (human skin malignant melanoma cells) at concentrations of 1 and 10 μmol·L^{-1}. The results are shown in Table 2. Remarkably, the anti-proliferative activities of all the compounds under investigation surpassed those of the established positive controls, *β*-elemene and 5-fluorouracil. Even more intriguing was the observation that intermediates **5** and **6** manifested superior anti-proliferative effects compared to *β*-elemene, indicating that the introduction of nitrogenous groups, specifically piperazine and 3-diazabicyclo[3.3.0]octane, into the molecular structure of *β*-elemene significantly bolsters its antitumor efficacy. On comparing the effects across the two concentrations, most compounds displayed a distinct selectivity toward K562 and CCRF-CEM cells over A375 and SK-MEL-2 cells. Based on these initial findings, compounds achieving inhibitory rates exceeding 85% were selected for further IC_{50} tests on K562 and CCRF-CEM cells.

As shown in Table 3, the anti-proliferative activity of most compounds increased significantly when NO donors were introduced. The IC_{50} values of **12a**, **12d**, **13a**, **13b**, **13d**, **13e**, and **13f** against K562 were less than 1 μmol·L^{-1}, and the IC_{50} values of **12d**, **13a**, **13b**, and **13e** against CCRF-CEM

Table 1 NO release levels of compounds in different time periods (mean ± SD, *n* = 3)

Compounds	Release levels of NO/μmol·L^{-1}						
	5 min	10 min	20 min	30 min	60 min	90 min	120 min
12a	1.62 ± 0.37	6.69 ± 0.41	9.20 ± 0.61	16.35 ± 0.22	29.35 ± 0.94	36.96 ± 0.41	45.39 ± 1.01
12b	0.26 ± 0.57	2.71 ± 0.00	5.11 ± 0.03	8.34 ± 0.05	10.94 ± 1.27	11.52 ± 0.70	16.50 ± 0.12
12c	0.26 ± 0.01	4.31 ± 0.25	5.07 ± 0.33	7.00 ± 0.45	12.10 ± 1.27	19.57 ± 1.02	25.33 ± 0.33
12d	1.77 ± 0.16	2.40 ± 0.16	4.28 ± 1.02	7.61 ± 0.33	16.56 ± 0.21	20.17 ± 1.23	27.47 ± 0.66
12e	1.10 ± 0.29	4.83 ± 0.82	12.82 ± 0.08	15.77 ± 1.31	21.77 ± 2.17	22.49 ± 0.08	15.92 ± 0.37
12f	1.42 ± 0.33	7.32 ± 0.08	7.87 ± 0.21	10.94 ± 0.78	17.54 ± 1.19	19.51 ± 1.02	19.60 ± 0.25
13a	1.30 ± 0.16	6.11 ± 1.56	13.58 ± 0.41	16.15 ± 1.35	24.17 ± 1.80	24.75 ± 1.39	30.30 ± 1.23
13b	0.84 ± 0.82	5.18 ± 0.49	5.85 ± 0.37	9.81 ± 0.98	16.44 ± 1.76	20.90 ± 1.51	30.13 ± 0.74
13c	0.42 ± 0.11	5.70 ± 0.49	11.98 ± 0.70	21.22 ± 0.25	24.08 ± 1.76	26.51 ± 0.94	18.81 ± 1.02
13d	2.84 ± 1.11	5.88 ± 0.98	11.66 ± 1.64	15.11 ± 1.51	23.76 ± 0.66	27.44 ± 1.68	34.59 ± 0.49
13e	1.45 ± 0.12	6.19 ± 0.37	12.48 ± 0.08	21.27 ± 1.64	26.69 ± 0.70	30.54 ± 2.05	33.69 ± 0.12
13f	0.64 ± 0.53	5.24 ± 0.16	12.39 ± 0.29	19.36 ± 0.49	22.61 ± 0.16	26.11 ± 0.70	30.33 ± 0.70

Table 2 Inhibitory rates (%) of compounds against four cell lines at different concentrations (1 and 10 μmol·L^{-1})

Compounds	K562		CCRF-CEM		A375		SK-MEL-2	
	1 μmol·L^{-1}	10 μmol·L^{-1}	1 μmol·L^{-1}	10 μmol·L^{-1}	1 μmol·L^{-1}	10 μmol·L^{-1}	1 μmol·L^{-1}	10 μmol·L^{-1}
β-Elemene	6.01	18.40	12.15	20.90	5.80	9.97	0.32	5.39
5	29.79	89.24	32.93	89.67	21.43	80.95	22.41	82.87
6	33.42	90.24	31.11	90.40	13.69	62.95	28.77	62.50
12a	87.23	90.24	80.44	92.35	48.36	81.10	20.37	82.65
12b	65.96	87.11	58.81	94.65	20.54	79.17	18.43	74.46
12c	75.47	91.11	67.31	91.98	17.71	79.46	14.01	68.97
12d	78.35	88.74	79.71	91.74	17.56	78.42	18.53	64.87
12e	25.53	88.49	18.96	91.74	4.61	51.19	8.30	48.81
12f	28.41	84.36	19.56	79.83	22.17	57.74	21.34	64.87
13a	80.30	93.24	87.75	90.93	54.50	82.65	62.23	83.32
13b	80.30	92.21	79.74	96.11	13.58	81.67	22.93	83.83
13c	69.19	91.52	59.25	84.92	22.26	79.87	18.73	66.53
13d	80.53	93.47	75.85	89.87	31.26	81.83	24.77	76.25
13e	77.55	92.21	76.21	94.70	30.77	81.01	20.16	80.76
13f	78.47	92.44	66.78	89.52	29.30	77.41	26.20	76.15
5-FU	47.42	76.17	52.18	78.21	25.04	59.41	30.09	68.99

Table 3 IC_{50} values of preferred compounds against K562 and CCRF-CEM cell lines (mean ± SEM, *n* = 3)

Compounds	IC_{50}/μmol·L^{-1}	
	K562	CCRF-CEM
β-Elemene	> 100	> 100
12a	0.88 ± 0.02	1.05 ± 0.02
12b	1.08 ± 0.04	1.21 ± 0.00
12c	1.06 ± 0.05	1.13 ± 0.01
12d	0.84 ± 0.01	0.98 ± 0.08
12e	4.96 ± 0.05	5.73 ± 0.06
13a	0.72 ± 0.01	0.78 ± 0.01
13b	0.83 ± 0.02	0.85 ± 0.02
13c	1.08 ± 0.02	1.07 ± 0.03
13d	0.48 ± 0.01	1.12 ± 0.03
13e	0.77 ± 0.02	0.79 ± 0.03
13f	0.85 ± 0.02	1.14 ± 0.04

were less than 1 μmol·L^{-1}. It was obvious that most of the selected compounds were more selective for K562 cells than for CCRF-CEM cells. We also found that the IC_{50} values of compounds with the 3-diazabicyclo[3.3.0]octane group were significantly better than those with the piperazine group against the K562 cell line. Overall, the introduction of NO donors further enhanced the antitumor activity of *β*-elemene. A direct correlation emerged between the the magnitude of NO release and the anti-proliferative potency of the compounds. Among these compounds, **13d** exhibited better activity and a higher NO release level.

Subsequent evaluations were conducted to assess the *in vitro* antitumor activity of compounds **6**, **10** and **10b** at a molar concentration ratio of 1 : 2, focusing specifically on the potential synergistic effect exhibited by compound **13d**. As illustrated in Fig. 3, the anti-proliferative activity of **13d** was 26-fold, 6-fold and 10-fold better than that of **6**, **10** and **10b**, respectively. It was even 3-4-fold more potent than the activity of their combinations in the molar ratio of 1 : 2. These findings underscore the potent *in vitro* antitumor activity inherent to compound **13d**. A plausible explanation for this enhanced potency might be the collaborative antitumor effects manifested through the synergistic antitumor effect of *β*-element and NO. This phenomenon of "1 + 2 > 3" indicated that compound **13d** displayed significant antitumor activity, and the *β*-elemene metabolites could still show potent antitumor activity after the NO release phase. Given these compelling *in vitro* results, compound **13d** is the primary candidate for subsequent *in vivo* pharmacodynamic evaluations.

Structure-activity relationship (SAR) analysis

The enhanced antitumor activity of *β*-elemene is attributed to the introduction of nitrogenous groups at positions 13 and 14 of *β*-elemene. A direct relationship was discerned between the antitumor activity and the extent of release of NO. The release levels of compounds **12a** and **13d** were

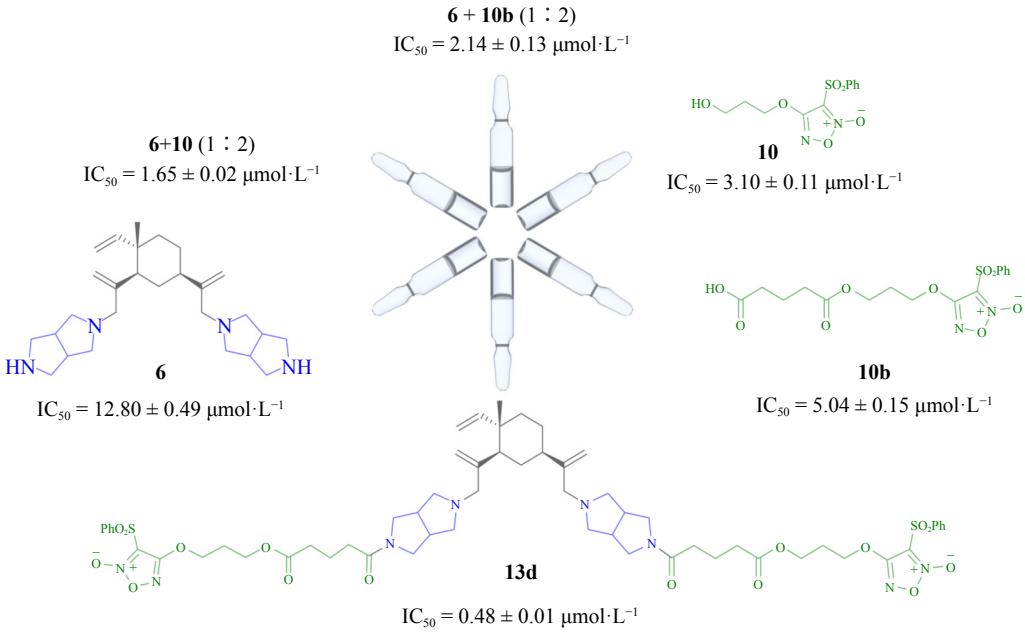

Fig. 3 Comparison of the anti-proliferative activity of compound 13d with those of 6, 10, 10b, and their combination in the molar ratio of 1 : 2 in K562 cells.

higher than those of **12b**, **12e**, **12f**, and **13c**, which may lead to their relatively weak antitumor activity. It was particularly noteworthy that derivatives containing a 3-diazabicyclol [3.3.0] octane group outperformed those embedded with a piperazine group in antitumor activities.Furthermore, an assessment of the alcohol chain length delineated a potency sequence as follows: propylene glycol > ethylene glycol > 1,4-butynediol (e.g., **13d** > **13a** > **13e**). Overall, glutaric anhydride exhibits more potent antitumor activity as a linker than butanedioic anhydride (e.g., **13d** > **13a**).

In vivo antitumor effect against leukemia

We assessed the *in vivo* antitumor activity of compound **13d** using a K562 xenograft tumor mouse model. Throughout the study, there was a consistent increase in the body weight of mice in the model, *β*-elemene, and compound **13d** groups, suggesting that *β*-elemene and compound **13d** do not exert any overt toxic effects on the mice (Fig. 4A). Within 28 days, the tumor volume in the model group also gradually in-

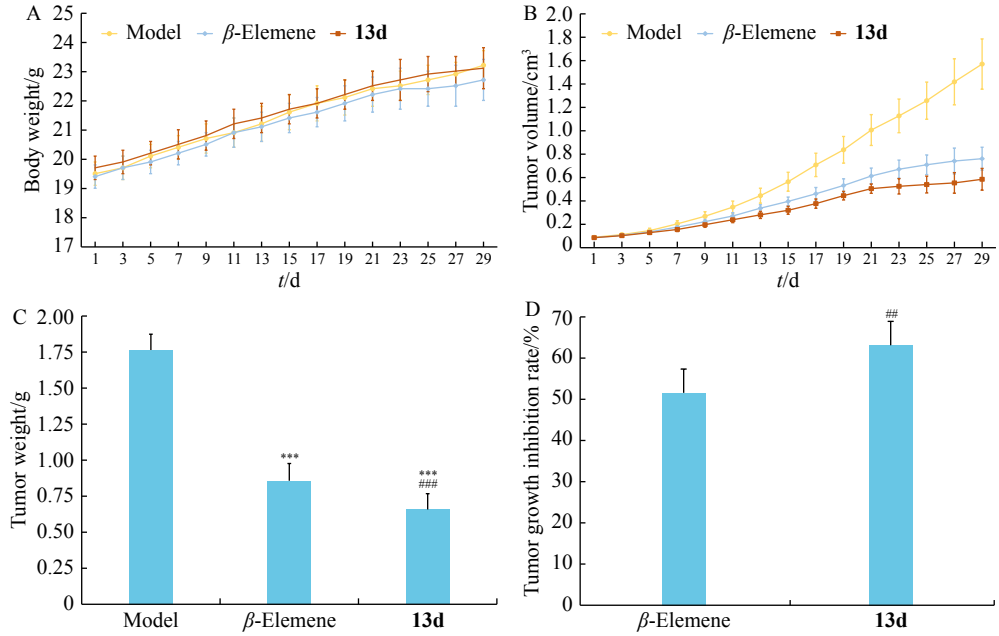

Fig. 4 *In vivo* antitumor activity of compound 13d in the K562 xenograft tumor mouse model (mean ± SD, *n* = 6). (A) Body weight; (B) Tumor volume (Day 13, 15, 17, 19, 21, 23, 27, and 29: $P < 0.05$; Day 25: $P < 0.01$, compound 13d group *vs* *β*-elemene group); (C) Tumor weight ($^{***}P < 0.001$ *vs* model group; $^{###}P < 0.001$ *vs* *β*-elemene group); (D) Tumor growth inhibition rate ($^{##}P < 0.01$ *vs* *β*-elemene group).

creased. However, such an increase was absent in the *β*-elemene and compound **13d** groups, implying a pronounced suppression of tumor growth in these two groups (Fig. 4B). At the end of the experiment, the tumor weight was much lower in the *β*-elemene and compound **13d** groups than in the model group (Fig. 4C). Both of them could inhibit tumor growth, but the inhibitory rate in the compound **13d** group was 11% more potent than that in the *β*-elemene group (Fig. 4D). These results collectively suggest that compound **13d** surpasses *β*-elemene exhibited in its *in vivo* antitumor efficacy.

Conclusions

A series of 13,14-disubstituted NO donor-*β*-elemene derivatives were designed and synthesized as potential agents for treating chronic myeloid leukemia according to the pharmacophore fusion strategy. All these designed compounds displayed strong NO release capabilities, translating to an enhanced antitumor activity *in vitro*. Among these, compound **13d** stood out, showcasing a dramatically improved IC_{50} value (0.48 μmol·L^{-1}) against the K562 cell line compared with that of *β*-elemene (IC_{50} > 100 μmol·L^{-1}). Furthermore, *in vivo* evaluations using the K562 xenograft tumor mouse model affirmed the superior antitumor efficacy of compound **13d**. It inhibited tumor growth effectively without manifesting noticeable toxic effects. In conclusion, these findings position compound **13d** as a promising candidate for leukemia treatment in the future.

Experimental

Chemistry

General information

Melting points were determined using an Agilent MPA100 digital melting point meter. Spectroscopic analysis was conducted using a Bruker Avance 500 spectrometer to record both ^{1}H (500 MHz) and ^{13}C (125 MHz) NMR spectral data. For these analyses, deuterated chloroform ($CDCl_3$) and deuterated dimethyl sulfoxide (DMSO-d_6) were utilized as the solvents, with tetramethylsilane (TMS) serving as the internal standard. Mass spectral data were acquired on two distinct instruments: the Agilent 1260 InfinityII/1625 for low-resolution spectra and the Agilent 1290-6530 Q-TOF instrument for high-resolution spectra.

*General synthetic procedures for **2***

A mixture of **1** (29.4 mmol), TBAF (1.0 mol·L^{-1} THF), dichloromethane (DCM), and acetic acid (HOAc) was stirred at 0 °C. Subsequently, NaClO solution (available chlorine ≥ 5.2 %) was added dropwise using a micro-injection pump within 5 h at 0 °C. The reaction was quenched by adding saturated $NaHCO_3$ until effervescence ceased. The mixture was then extracted with ethyl acetate (EA), and the resultant organic layer was washed sequentially with water and brine. After drying over anhydrous Na_2SO_4, the solvent was evaporated under vacuum. The residue underwent column chromatography with petroleum ether as the eluent, yielding compound **2** (25%) as a colorless liquid.

^{1}H NMR (500 MHz, $CDCl_3$) δ: 5.79 (dd, *J* = 17.2, 11.0 Hz, 1H), 5.28 (s, 1H), 5.18 (s, 1H), 5.04 (s, 1H), 4.97–4.89 (m, 3H), 4.11 (s, 3H), 3.97 (d, *J* = 11.7 Hz, 1H), 2.35–2.22 (m, 2H), 1.77–1.42 (m, 9H), 0.99 (s, 3H); ^{13}C NMR (125 MHz, $CDCl_3$) δ: 149.51, 148.95, 147.44, 116.29, 113.33, 111.42, 50.88, 47.63, 47.56, 41.01, 39.72, 39.61, 33.76, 26.97, 15.73.

*General synthetic procedures for intermediates **3** and **4***

A mixture of compound **2** (1.0 mmol), Cs_2CO_3 (3.0 mmol), and the corresponding Boc-protected piperazine or 3-diazabicyclo[3.3.0]octane (3.0 mmol) was dissolved in DMF (6 mL). The resulting solution was stirred at 60 °C overnight. Upon completion, the reaction was quenched with water at room temperature, and the resulting solution was extracted with EA. The separated organic layer was sequentially washed with water and brine. Following drying over Na_2SO_4, the solvent was removed under vacuum. The crude product was purified *via* column chromatography (DCM/MeOH 100∶1, *V*/*V*) to obtain intermediates **3** and **4** as liquids.

4,4'-(((1*R*,3*R*,4*S*)-4-Methyl-4-vinylcyclohexane-1,3-diyl) bis(prop-2-ene-2,1-diyl))bis(piperazine-1-carboxylate) (**3**)

Light yellow liquid, yield 58%. ^{1}H NMR (500 MHz, $CDCl_3$) δ: 5.8 (dd, *J* = 10.8, 17.5 Hz, 1H), 5.0 (s, 1H), 4.9–4.8 (m, 4H), 4.8 (s, 1H), 3.4 (s, 8H), 3.1–2.6 (m, 4H), 2.4–2.2 (m, 9H), 2.1 (t, *J* = 11.5 Hz, 1H), 1.4 (s, 24H), 1.0 (s, 3H); ^{13}C NMR (125 MHz, $CDCl_3$) δ: 154.9, 154.9, 150.6, 150.6, 150.1, 113.8, 111.3, 110.3, 79.6, 66.4, 63.6, 53.1, 53.0, 48.2, 42.4, 40.1, 40.0, 34.0, 28.5, 28.5, 27.2, 16.0. ESI-MS *m/z* 573.4 $[M + H]^+$.

5,5'-(((1*R*,3*R*,4*S*)-4-Methyl-4-vinylcyclohexane-1,3-diyl)bis(prop-2-ene-2,1-diyl))bis(hexahydropyrrolo[3,4-c]pyrrole-2(*1H*)-carboxylate) (**4**)

Brown liquid, yield 68%. ^{1}H NMR (500 MHz, $CDCl_3$) δ: 5.8 (dd, *J* = 10.8, 17.5 Hz, 1H), 5.1 (s, 1H), 5.0–4.8 (m, 4H), 4.7 (s, 1H), 3.6–3.5 (m, 4H), 3.2 (s, 5H), 3.1–2.9 (m, 2H), 2.8–2.7 (m, 5H), 2.6–2.5 (m, 3H), 2.4–2.3 (m, 4H), 2.2 (d, *J* = 11.6 Hz, 1H), 2.0 (d, *J* = 19.2 Hz, 2H), 1.4 (s, 25H), 1.0 (s, 3H). ^{13}C NMR (125 MHz, $CDCl_3$) δ: 154.4, 151.8, 150.1, 149.4, 112.8, 110.2, 109.9, 79.1, 63.0, 60.3, 60.2, 60.0, 51.6, 48.5, 42.7, 42.1, 41.3, 40.0, 39.9, 34.1, 28.6, 27.2, 16.0. ESI-MS *m/z* 625.4 $[M + H]^+$.

*General synthetic procedures for intermediates **5** and **6***

Compound **3** (1.0 mmol) was dissolved in MeOH (4 mL). A 1,4-dioxane hydrochloride solution (4 mol·L^{-1}) was then added dropwise. The reaction mixture was stirred at 0 °C overnight. Following the reaction, the solvent was removed under reduced pressure. The resultant residue was neutralized with saturated $NaHCO_3$ and subsequently extracted with DCM. The organic layer was separated, washed with water and brine, dried over Na_2SO_4, and concentrated *in vacuo*. Compounds **5**–**6** were obtained as liquids.

1,1'-(((1*R*,3*R*,4*S*)-4-Methyl-4-vinylcyclohexane-1,3-diyl)bis(prop-2-ene-2,1-diyl))dipiperazine (**5**)

Light yellow liquid, yield 97%. ^{1}H NMR (500 MHz,

DMSO-d_6) δ: 5.8 (dd, *J* = 10.7, 17.5 Hz, 1H), 5.0 (s, 1H), 5.0–4.8 (m, 4H), 4.8 (s, 1H), 3.0 (d, *J* = 13.6 Hz, 1H), 2.8 (d, *J* = 44.3 Hz, 10H), 2.6 (d, *J* = 13.6 Hz, 1H), 2.4–2.1 (m, 9H), 2.1–2.0 (m, 1H), 1.6 (dt, *J* = 11.8, 27.2 Hz, 2H), 1.5–1.3 (m, 4H), 1.0 (s, 3H); ^{13}C NMR (125 MHz, $CDCl_3$) δ: 150.6, 150.1, 148.1, 114.0, 111.1, 110.2, 67.0, 64.2, 53.9, 53.8, 48.1, 45.6, 42.1, 39.9, 34.1, 27.2, 16.0. ESI-MS *m/z* 373.2 $[M + H]^+$.

2,2'-(((1*R*,3*R*,4*S*)-4-Methyl-4-vinylcyclohexane-1,3-diyl)bis(prop-2-ene-2,1-diyl))bis(octahydropyrrolo[3,4-c]pyrrole) (**6**)

Brown liquid, yield 95 %. ^{1}H NMR (500 MHz, $CDCl_3$) δ: 5.8 (dd, *J* = 10.8, 17.5 Hz, 1H), 5.0 (s, 1H), 4.9–4.8 (m, 4H), 4.7 (s, 1H), 3.5–3.3 (m, 4H), 3.1 (d, *J* = 12.2 Hz, 1H), 3.0–2.8 (m, 8H), 2.8–2.6 (m, 6H), 2.5–2.4 (m, 2H), 2.3 (dd, *J* = 5.8, 9.2 Hz, 1H), 2.2–2.1 (m, 3H), 2.0 (dd, *J* = 5.4, 9.3 Hz, 1H), 1.7–1.4 (m, 6H), 1.0 (s, 3H); ^{13}C NMR (125 MHz, $CDCl_3$) δ: 152.0, 150.1, 149.8, 113.6, 110.4, 110.3, 76.9, 63.3, 60.2, 59.4, 59.3, 58.7, 53.5, 53.3, 52.9, 52.3, 47.2, 42.0, 41.8, 41.6, 40.8, 40.0, 39.9, 34.1, 27.6, 15.7. ESI-MS *m/z* 425.4 $[M + H]^+$.

General synthetic procedures for compounds ***9*–*11***

Compounds **9**–**11** were synthesized following the methods previously described [25].

General synthetic procedures for compounds ***12a*–*12f*** *and* ***13a*–*13f***

NO donor intermediates **9a**–**b**, **10a**–**b**, or **11a**–**b** (0.2 mmol), DIPEA (0.8 mmol), EDCI (0.4 mmol), and HOBt (0.2 mmol) were added to a solution of *β*-elemene intermediate **5** or **6** (0.1 mmol) in anhydrous DCM (3 mL). This reaction mixture was stirred at room temperature overnight. Afterward, it was diluted with DCM. The organic layers were then separated and washed sequentially with water and brine before being dried over Na_2SO_4. The concentrated residue, obtained under reduced pressure, was further purified *via* column chromatography (DCM/MeOH 60∶1, *V*/*V*), yielding 12a-f and 13a-f in liquid form.

4-(2-((4-(4-(2-((1*R*,3*R*,4*S*)-4-Methyl-3-(3-(4-(4-(2-((2-oxido-3-(phenyl sulfonyl)-1,2,5-oxadiazol-4-yl)oxy)ethoxy)-4-oxobutanoyl)piperazin-1-yl)prop-1-en-2-yl)-4-vinylcyclohexyl)allyl)piperazin-1-yl)-4-oxobutanoyl)oxy)ethoxy)-3-(phenyl sulfonyl)-1,2,5-oxadiazole 2-oxide (**12a**)

Colorless transparent liquid, yield 54%. ^{1}H NMR (500 MHz, $CDCl_3$) δ: 8.04 (d, *J* = 7.7 Hz, 4H), 7.76 (t, *J* = 7.5 Hz, 2H), 7.62 (t, *J* = 7.8 Hz, 4H), 5.77 (dd, *J* = 10.8, 17.5 Hz, 1H), 5.03 (s, 1H), 4.93–4.83 (m, 4H), 4.78 (s, 1H), 4.65–4.59 (m, 4H), 4.53–4.46 (m, 4H), 3.57 (s, 4H), 3.44 (s, 4H), 3.02 (d, *J* = 13.8 Hz, 1H), 2.90 (q, *J* = 13.4 Hz, 2H), 2.63 (d, *J* = 13.9 Hz, 1H), 2.48 (t, *J* = 7.0 Hz, 4H), 2.40 (s, 4H), 2.34 (s, 4H), 2.25 (s, 2H), 2.01–1.95 (m, 4H), 1.60 (d, *J* = 12.4 Hz, 2H), 1.46 (dd, *J* = 13.5, 26.4 Hz, 4H), 0.98 (s, 3H); ^{13}C NMR (125 MHz, $CDCl_3$) δ: 173.0, 169.5, 169.5, 158.8, 150.4, 150.1, 148.1, 138.1, 135.8, 129.8, 128.7, 114.0, 111.4, 110.5, 110.4, 69.0, 66.1, 63.4, 61.3, 53.3, 53.2, 52.9, 52.9, 48.2, 45.4, 42.4, 42.0, 40.1, 40.0, 34.0, 29.3, 28.0, 27.2, 26.5, 16.0. HR-ESI-MS *m/z* 1109.3953 (Calcd. for $C_{51}H_{64}N_8O_{16}S_2$ $[M + H]^+$, 1109.3954).

4-(3-((4-(4-(2-((*1R*,*3R*,*4S*)-4-Methyl-3-(3-(4-(4-(3-((2-oxido-3-(phenyl sulfonyl)-1,2,5-oxadiazol-4-yl)oxy)propoxy)-4-oxobutanoyl)piperazin-1-yl)prop-1-en-2-yl)-4-vinylcyclohexyl)allyl)piperazin-1-yl)-4-oxobutanoyl)oxy)propoxy)-3-(phenylsulfonyl)-1,2,5-oxadiazole 2-oxide (**12b**)

Colorless transparent liquid, yield 49%. ^{1}H NMR (500 MHz, $CDCl_3$) δ: 8.10–8.02 (m, 4H), 7.75 (t, *J* = 7.5 Hz, 2H), 7.63 (t, *J* = 7.9 Hz, 4H), 5.79 (dd, *J* = 10.9, 17.2 Hz, 1H), 5.06 (s, 1H), 4.97–4.85 (m, 4H), 4.81 (s, 1H), 4.52 (t, *J* = 6.1 Hz, 4H), 4.29 (t, *J* = 6.0 Hz, 4H), 3.50 (d, *J* = 47.0 Hz, 8H), 3.04 (d, *J* = 13.0 Hz, 1H), 2.92 (q, *J* = 13.0, 13.6 Hz, 2H), 2.64 (s, 9H), 2.36 (d, *J* = 17.6 Hz, 6H), 2.26–2.18 (m, 6H), 2.04 (d, *J* = 34.2 Hz, 2H), 1.63 (s, 2H), 1.53–1.40 (m, 4H), 0.99 (s, 3H); ^{13}C NMR (125 MHz, $CDCl_3$) δ: 173.2, 173.2, 169.6, 169.5, 159.0, 150.3, 150.0, 148.0, 138.1, 135.7, 129.8, 128.7, 114.0, 111.5, 110.6, 110.4, 68.2, 66.1, 63.4, 60.4, 53.3, 53.2, 52.9, 52.8, 48.2, 45.4, 42.4, 41.9, 40.1, 40.0, 34.0, 29.3, 28.1, 28.0, 27.2, 16.0. HR-ESI-MS *m/z* 1137.4261 (Calcd. for $C_{53}H_{68}N_8O_{16}S_2$ $[M + H]^+$, 1137.4267).

4-(2-((5-(4-(2-((*1R*,*3R*,*4S*)-4-Methyl-3-(3-(4-(5-(2-((2-oxido-3-(phenyl sulfonyl)-1,2,5-oxadiazol-4-yl)oxy)ethoxy)-5-oxopentanoyl)piperazin-1-yl)prop-1-en-2-yl)-4-vinylcyclohexyl)allyl)piperazin-1-yl)-5-oxopentanoyl)oxy)ethoxy)-3-(phenyl sulfonyl)-1,2,5-oxadiazole 2-oxide (**12c**)

Colorless transparent liquid, yield 30%. ^{1}H NMR (500 MHz, $CDCl_3$) δ: 8.07–8.00 (m, 4H), 7.76 (t, *J* = 7.5 Hz, 2H), 7.63 (t, *J* = 7.9 Hz, 4H), 5.78 (dd, *J* = 10.8, 17.3 Hz, 1H), 5.04 (s, 1H), 4.95–4.84 (m, 4H), 4.79 (s, 1H), 4.65–4.59 (m, 4H), 4.52–4.47 (m, 4H), 3.58 (s, 4H), 3.44 (s, 4H), 3.07–2.99 (m, 1H), 2.90 (q, *J* = 12.2, 13.1 Hz, 2H), 2.64 (d, *J* = 13.8 Hz, 1H), 2.48 (t, *J* = 6.9 Hz, 4H), 2.40 (td, *J* = 2.7, 7.4 Hz, 5H), 2.34 (s, 5H), 2.22 (dd, *J* = 10.1, 17.7 Hz, 4H), 2.00–1.96 (m, 4H), 1.64–1.58 (m, 2H), 1.52–1.40 (m, 4H), 0.98 (s, 3H); ^{13}C NMR (125 MHz, $CDCl_3$) δ: 173.2, 170.6, 170.6, 158.8, 150.4, 150.1, 148.1, 138.1, 135.8, 129.8, 128.7, 114.0, 111.4, 110.5, 110.4, 69.1, 66.2, 63.4, 61.1, 53.4, 53.4, 53.0, 53.0, 48.3, 45.6, 42.4, 41.8, 40.1, 40.0, 34.0, 33.3, 32.2, 27.3, 20.3, 16.0. HR-ESI-MS *m/z* 1137.4262 (Calcd. for $C_{53}H_{68}N_8O_{16}S_2$ $[M + H]^+$, 1137.4267).

4-(3-((5-(4-(2-((*1R*,*3R*,*4S*)-4-Methyl-3-(3-(4-(5-(3-((2-oxido-3-(phenyl sulfonyl)-1,2,5-oxadiazol-4-yl)oxy)propoxy)-5-oxopentanoyl)piperazin-1-yl)prop-1-en-2-yl)-4-vinylcyclohexyl)allyl)piperazin-1-yl)-5-oxopentanoyl)oxy)propoxy)-3-(phenylsulfonyl)-1,2,5-oxadiazole 2-oxide (**12d**)

Colorless transparent liquid, yield 49%. ^{1}H NMR (500 MHz, $CDCl_3$) δ: 8.10–8.01 (m, 4H), 7.76 (t, *J* = 7.5 Hz, 2H), 7.63 (t, *J* = 7.9 Hz, 4H), 5.79 (dd, *J* = 10.9, 16.9 Hz, 1H), 5.05 (s, 1H), 4.97–4.77 (m, 5H), 4.50 (t, *J* = 6.1 Hz, 4H), 4.26 (t, *J* = 6.1 Hz, 4H), 3.64–3.38 (m, 8H), 3.08–3.01 (m, 1H), 2.92 (q, *J* = 13.1 Hz, 2H), 2.69–2.62 (m, 1H), 2.45–2.32 (m, 14H), 2.26 (d, *J* = 8.7 Hz, 2H), 2.23–2.19 (m, 4H), 1.98–1.92 (m, 6H), 1.66–1.59 (m, 2H), 1.45 (dd, *J* = 11.9, 22.8 Hz, 4H), 0.99 (s, 3H); ^{13}C NMR (125 MHz, $CDCl_3$) δ: 173.3, 170.6,

159.0, 150.4, 150.1, 148.1, 138.1, 135.8, 129.8, 128.7, 114.0, 111.4, 110.6, 110.4, 68.1, 66.2, 63.4, 60.3, 53.4, 53.4, 53.0, 52.9, 48.3, 45.7, 42.4, 41.8, 40.1, 40.0, 34.0, 33.4, 32.3, 28.1, 27.3, 20.5, 16.0. HR-ESI-MS *m/z* 1165.4582 (Calcd. for $C_{55}H_{72}N_8O_{16}S_2$ $[M + H]^+$, 1165.458).

4-((4-((4-(4-(2-((*1R*,*3R*,*4S*)-4-Methyl-3-(3-(4-(4-((4-((2-oxido-3-(phenyl sulfonyl)-1,2,5-oxadiazol-4-yl)oxy)but-2-yn-1-yl)oxy)-4-oxobutanoyl)piperazin-1-yl)prop-1-en-2-yl)-4-vinylcyclohexyl)allyl)piperazin-1-yl)-4-oxobutanoyl)oxy)but-2-yn-1-yl)oxy)-3-(phenylsulfonyl)-1,2,5-oxadiazole 2-oxide (**12e**)

Colorless transparent liquid, yield 32%. ^{1}H NMR (500 MHz, $CDCl_3$) δ: 8.11–8.05 (m, 4H), 7.78–7.74 (m, 2H), 7.67–7.61 (m, 4H), 5.79 (dd, *J* = 10.8, 17.4 Hz, 1H), 5.09 (t, *J* = 1.6 Hz, 4H), 5.06–4.79 (m, 6H), 4.74 (d, *J* = 8.7 Hz, 4H), 3.71–3.40 (m, 8H), 3.13–2.87 (m, 3H), 2.72–2.61 (m, 9H), 2.47–2.25 (m, 8H), 2.23–2.16 (m, 1H), 2.13–2.03 (m, 1H), 1.61 (d, *J* = 11.9 Hz, 2H), 1.55–1.39 (m, 4H), 0.99 (s, 3H); ^{13}C NMR (125 MHz, $CDCl_3$) δ: 172.5, 169.4, 158.0, 150.0, 150.0, 148.0, 138.0, 135.9, 129.8, 128.8, 111.6, 111.5, 110.7, 110.5, 84.2, 78.6, 66.1, 66.1, 63.4, 63.4, 61.0, 61.0, 58.8, 53.6, 53.2, 53.2, 52.9, 52.8, 52.1, 48.3, 45.4, 42.4, 42.0, 40.1, 40.0, 34.0, 29.2, 27.9, 27.2, 16.0. HR-ESI-MS *m/z* 1157.3954 (Calcd. for $C_{55}H_{64}N_8O_{16}S_2$ $[M + H]^+$, 1157.3954).

4-((4-((5-(4-(2-((*1R*,*3R*,*4S*)-4-Methyl-3-(3-(4-(5-((4-((2-oxido-3-(phenyl sulfonyl)-1,2,5-oxadiazol-4-yl)oxy)but-2-yn-1-yl)oxy)-5-oxopentanoyl)piperazin-1-yl)prop-1-en-2-yl)-4-vinylcyclohexyl)allyl)piperazin-1-yl)-5-oxopentanoyl)oxy)but-2-yn-1-yl)oxy)-3-(phenylsulfonyl)-1,2,5-oxadiazole 2-oxide (**12f**)

Colorless transparent liquid, yield 26%. ^{1}H NMR (500 MHz, $CDCl_3$) δ: 8.12–8.04 (m, 4H), 7.77 (t, *J* = 7.5 Hz, 2H), 7.64 (t, *J* = 7.9 Hz, 4H), 5.80 (dd, *J* = 11.3, 16.4 Hz, 1H), 5.10 (s, 5H), 5.00–4.77 (m, 5H), 4.74 (s, 4H), 3.70–3.34 (m, 8H), 3.05 (dd, *J* = 2.8, 13.5 Hz, 1H), 2.99–2.86 (m, 2H), 2.66 (dd, *J* = 5.3, 12.4 Hz, 1H), 2.46 (t, *J* = 6.9 Hz, 4H), 2.39 (dd, *J* = 4.6, 9.8 Hz, 7H), 2.31–2.14 (m, 4H), 2.11–2.05 (m, 1H), 1.97 (ddt, *J* = 3.7, 7.2, 14.3 Hz, 6H), 1.66–1.59 (m, 2H), 1.53–1.39 (m, 4H), 0.99 (s, 3H); ^{13}C NMR (125 MHz, $CDCl_3$) δ: 172.6, 170.5, 158.0, 150.3, 150.0, 148.0, 137.9, 135.9, 129.8, 129.1, 128.7, 114.0, 111.5, 110.7, 110.4, 84.1, 78.6, 66.1, 63.4, 61.0, 58.7, 53.6, 53.4, 53.4, 53.0, 52.9, 51.9, 48.2, 45.6, 42.4, 41.8, 40.1, 40.0, 34.0, 33.2, 32.1, 27.2, 20.3, 16.0. HR-ESI-MS *m/z* 1185.4271 (Calcd. for $C_{57}H_{68}N_8O_{16}S_2$ $[M + H]^+$, 1185.4267).

4-(2-((4-(5-(2-((*1R*,*3R*,*4S*)-4-Methyl-3-(3-(5-(4-(2-((2-oxido-3-(phenyl sulfonyl)-1,2,5-oxadiazol-4-yl)oxy)ethoxy)-4-oxobutanoyl)hexahydropyrrolo[3,4-c]pyrrol-2(*1H*)-yl)prop-1-en-2-yl)-4-vinylcyclohexyl)allyl)hexahydropyrrolo[3,4-c]pyrrol-2(*1H*)-yl)-4-oxobutanoyl)oxy)ethoxy)-3-(phenylsulfonyl)-1,2,5-oxadiazole 2-oxide (**13a**)

Colorless transparent liquid, yield 50%. ^{1}H NMR (500 MHz, $CDCl_3$) δ: 8.10–8.03 (m, 4H), 7.76 (t, *J* = 7.5 Hz, 2H), 7.63 (t, *J* = 7.9 Hz, 4H), 5.77 (dd, *J* = 11.0, 16.8 Hz, 1H), 5.06 (s, 1H), 4.97–4.83 (m, 4H), 4.74 (s, 1H), 4.65–4.60 (m, 4H), 4.51 (dt, *J* = 3.6, 6.9 Hz, 4H), 3.76–3.64 (m, 4H), 3.43–3.25 (m, 4H), 3.16 (s, 1H), 3.00 (s, 2H), 2.88 (s, 2H), 2.79–2.68 (m, 5H), 2.63–2.54 (m, 5H), 2.50–2.33 (m, 7H), 2.18–1.96 (m, 4H), 1.64–1.56 (m, 2H), 1.54–1.40 (m, 4H), 0.96 (s, 3H); ^{13}C NMR (125 MHz, $CDCl_3$) δ: 173.0, 169.2, 158.8, 151.6, 150.1, 150.0, 138.2, 135.8, 129.8, 128.7, 113.0, 110.5, 110.4, 110.1, 109.9, 69.1, 62.9, 62.8, 61.4, 61.3, 60.3, 60.2, 60.2, 60.0, 53.6, 52.4, 51.5, 48.8, 48.6, 42.5, 42.5, 42.4, 40.6, 40.6, 40.0, 39.9, 34.0, 29.4, 29.1, 27.4, 16.1. HR-ESI-MS *m/z* 1161.4258 (Calcd. for $C_{55}H_{68}N_8O_{16}S_2$ $[M + H]^+$, 1161.4267).

4-(3-((4-(5-(2-((*1R*,*3R*,*4S*)-4-Methyl-3-(3-(5-(4-(3-((2-oxido-3-(phenyl sulfonyl)-1,2,5-oxadiazol-4-yl)oxy)propoxy)-4-oxobutanoyl)hexahydropyrrolo [3,4-c]pyrrol-2(*1H*)-yl)prop-1-en-2-yl)-4vinylcyclohexyl)allyl)hexahydropyrrolo[3,4-c]pyrrol-2(*1H*)-yl)-4-oxobutanoyl)oxy)propoxy)-3-(phenylsulfonyl)-1,2,5-oxadiazole 2-oxide (**13b**)

Light yellow liquid, yield 59%. ^{1}H NMR (500 MHz, $CDCl_3$) δ: 8.05 (d, *J* = 7.5 Hz, 4H), 7.75 (t, *J* = 7.5 Hz, 2H), 7.62 (t, *J* = 7.9 Hz, 4H), 5.77 (ddd, *J* = 2.7, 10.8, 17.2 Hz, 1H), 5.06 (s, 1H), 4.94 (s, 1H), 4.89–4.83 (m, 3H), 4.74 (s, 1H), 4.51 (t, *J* = 6.1 Hz, 4H), 4.28 (q, *J* = 5.6 Hz, 4H), 3.67 (q, *J* = 7.1, 8.2 Hz, 4H), 3.37–3.25 (m, 4H), 3.21–3.11 (m, 1H), 3.00 (s, 2H), 2.88 (s, 2H), 2.80–2.74 (m, 2H), 2.71–2.53 (m, 12H), 2.48–2.36 (m, 5H), 2.21 (p, *J* = 6.1 Hz, 4H), 2.16–2.09 (m, 1H), 2.07–2.00 (m, 1H), 1.64–1.56 (m, 2H), 1.52–1.38 (m, 4H), 0.96 (s, 3H); ^{13}C NMR (125 MHz, $CDCl_3$) δ: 173.2, 169.3, 159.0, 150.1, 150.0, 149.9, 138.1, 135.7, 129.8, 128.7, 110.7, 110.6, 110.5, 110.4, 110.4, 68.2, 62.9, 62.8, 62.8, 60.4, 60.1, 60.1, 59.9, 52.2, 52.2, 51.4, 51.3, 48.5, 42.4, 42.4, 42.3, 40.5, 40.5, 40.5, 39.9, 34.0, 29.4, 29.1, 28.1, 27.3, 15.9. HR-ESI-MS *m/z* 1189.4585 (Calcd. for $C_{57}H_{72}N_8O_{16}S_2$ $[M + H]^+$, 1189.458).

4-(2-((5-(5-(2-((*1R*,*3R*,*4S*)-4-Methyl-3-(3-(5-(5-(2-((2-oxido-3-(phenyl sulfonyl)-1,2,5-oxadiazol-4-yl)oxy)ethoxy)-5-oxopentanoyl)hexahydropyrrolo[3,4-c]pyrrol-2(*1H*)-yl)prop-1-en-2-yl)-4-vinylcyclohexyl)allyl)hexahydropyrrolo[3,4-c]pyrrol-2(*1H*)-yl)-5-oxopentanoyl)oxy)ethoxy)-3-(phenylsulfonyl)-1,2,5-oxadiazole 2-oxide (**13c**)

Colorless transparent liquid, yield 71%. ^{1}H NMR (500 MHz, $CDCl_3$) δ: 8.05 (d, *J* = 7.6 Hz, 4H), 7.76 (t, *J* = 7.5 Hz, 2H), 7.63 (t, *J* = 7.9 Hz, 4H), 5.76 (ddd, *J* = 2.9, 10.8, 17.1 Hz, 1H), 5.05 (s, 1H), 4.95–4.82 (m, 4H), 4.73 (s, 1H), 4.62 (t, *J* = 4.5 Hz, 4H), 4.50 (q, *J* = 4.0 Hz, 4H), 3.73–3.59 (m, 4H), 3.44–3.24 (m, 4H), 3.21–3.11 (m, 1H), 3.00 (s, 2H), 2.92–2.83 (m, 2H), 2.77 (s, 2H), 2.68 (d, *J* = 14.3 Hz, 1H), 2.63–2.53 (m, 3H), 2.48 (t, *J* = 7.1 Hz, 4H), 2.42 (s, 2H), 2.37–2.30 (m, 7H), 2.16–2.09 (m, 1H), 1.99 (dt, *J* = 4.7, 9.2 Hz, 5H), 1.63–1.38 (m, 6H), 0.96 (s, 3H); ^{13}C NMR (125 MHz, $CDCl_3$) δ: 173.2, 170.4, 158.8, 150.9, 150.0, 149.9, 138.1, 135.8, 129.9, 128.7, 110.8, 110.5, 110.5, 110.5, 110.0, 69.1, 62.9, 62.8, 61.2, 61.1, 60.1, 60.0, 60.0, 59.9, 53.6, 52.2, 52.2, 51.2, 48.5, 42.5, 42.4, 42.3, 42.3, 40.5, 40.5, 39.9, 33.9, 33.6, 33.3, 27.3, 20.0, 16.0. HR-ESI-MS *m/z* 1189.4583 (Calcd. for $C_{57}H_{72}N_8O_{16}S_2$ $[M + H]^+$, 1189.458).

4-(3-((5-(5-(2-((*1R*,*3R*,*4S*)-4-Methyl-3-(3-(5-(5-(3-((2-oxido-3-(phenyl sulfonyl)-1,2,5-oxadiazol-4-yl)oxy)propoxy)-5-oxopentanoyl)hexahydropyrrolo[3,4-c]pyrrol-2(*1H*)-yl)prop-1-en-2-yl)-4-vinylcyclohexyl)allyl)hexahydropyrrolo[3,4-c]pyrrol-2(*1H*)-yl)-5-oxopentanoyl)oxy)propoxy)-3-(phenylsulfonyl)-1,2,5-oxadiazole 2-oxide (**13d**)

Colorless transparent liquid, yield 63%. ^{1}H NMR (500 MHz, $CDCl_3$) δ: 8.08–8.00 (m, 4H), 7.75 (t, *J* = 7.5 Hz, 2H), 7.61 (t, *J* = 7.9 Hz, 4H), 5.80–5.70 (m, 1H), 5.05 (s, 1H), 4.93 (s, 1H), 4.89–4.81 (m, 3H), 4.73 (s, 1H), 4.49 (t, *J* = 6.1 Hz, 4H), 4.25 (t, *J* = 6.1 Hz, 4H), 3.66 (dt, *J* = 9.9, 29.9 Hz, 4H), 3.41–3.25 (m, 4H), 3.08–2.50 (m, 16H), 2.41 (t, *J* = 7.2 Hz, 6H), 2.30 (t, *J* = 7.3 Hz, 4H), 2.22–2.17 (m, 4H), 1.97–1.91 (m, 4H), 1.57 (s, 2H), 1.49–1.38 (m, 4H), 0.95 (s, 3H); ^{13}C NMR (125 MHz, $CDCl_3$) δ: 173.3, 170.4, 158.9, 150.1, 150.0, 149.9, 138.1, 135.8, 129.8, 128.6, 110.6, 110.5, 110.5, 110.4, 110.4, 68.1, 62.9, 62.8, 60.2, 60.1, 60.0, 60.0, 59.9, 52.4, 51.3, 51.3, 48.8, 48.5, 42.8, 42.5, 42.4, 42.4, 40.5, 40.5, 39.9, 33.7, 33.6, 33.5, 28.0, 27.2, 20.1, 16.0. HR-ESI-MS *m/z* 1217.4898 (Calcd. for $C_{59}H_{76}N_8O_{16}S_2$ $[M + H]^+$, 1217.4893).

4-((4-((4-(5-(2-((*1R*,*3R*,*4S*)-4-Methyl-3-(3-(5-(4-((4-((2-oxido-3-(phenyl sulfonyl)-1,2,5-oxadiazol-4-yl)oxy)but-2-yn-1-yl)oxy)-4-oxobutanoyl)hexahydropyrrolo[3,4-c]pyrrol-2(*1H*)-yl)prop-1-en-2-yl)-4-vinylcyclohexyl) allyl)hexahydropyrrolo[3,4-c]pyrrol-2(*1H*)-yl)-4-oxobutanoyl)oxy)but-2-yn-1-yl)oxy) -3-(phenylsulfonyl)-1,2,5-oxadiazole 2-oxide (**13e**)

Colorless transparent liquid, yield 46%. ^{1}H NMR (500 MHz, $CDCl_3$) δ: 8.09 (dd, *J* = 8.1, 16.0 Hz, 4H), 7.79–7.74 (m, 2H), 7.64 (t, *J* = 7.0 Hz, 4H), 5.83–5.73 (m, 1H), 5.12–5.07 (m, 4H), 5.05–4.82 (m, 6H), 4.75 (d, *J* = 8.3 Hz, 4H), 3.74–3.64 (m, 4H), 3.44–3.31 (m, 4H), 3.05 (d, *J* = 9.6 Hz, 2H), 2.92 (d, *J* = 16.1 Hz, 2H), 2.82 (d, *J* = 11.3 Hz, 2H), 2.75–2.67 (m, 6H), 2.59 (s, 6H), 2.53–2.42 (m, 4H), 2.33–1.99 (m, 4H), 1.62–1.41 (m, 6H), 0.97 (s, 3H); ^{13}C NMR (125 MHz, $CDCl_3$) δ: 172.5, 169.1, 158.0, 150.1, 150.0, 149.1, 138.0, 135.9, 129.8, 128.8, 110.9, 110.7, 110.4, 110.3, 110.1, 84.2, 78.6, 62.8, 60.2, 58.8, 53.6, 52.4, 52.1, 51.5, 48.8, 48.5, 42.8, 42.5, 42.4, 41.6, 40.6, 40.0, 39.9, 34.0, 29.3, 29.0, 27.4, 16.0. HR-ESI-MS *m/z* 1209.4269 (Calcd. for $C_{59}H_{68}N_8O_{16}S_2$ $[M + H]^+$, 1209.4267).

4-((4-((5-(5-(2-((*1R*,*3R*,*4S*)-4-Methyl-3-(3-(5-(5-((4-((2-oxido-3-(phenyl sulfonyl)-1,2,5-oxadiazol-4-yl)oxy)but-2-yn-1-yl) oxy)-5-oxopentanoyl) hexahydropyrrolo[3,4-c]pyrrol-2(*1H*)-yl)prop-1-en-2-yl)-4-vinylcyclohexyl) allyl)hexahydropyrrolo[3,4-c]pyrrol-2(*1H*)-yl)-5-oxopentanoyl)oxy)but-2-yn-1-yl) oxy)-3-(phenylsulfonyl)-1,2,5-oxadiazole 2-oxide (**13f**)

Colorless transparent liquid, yield 49%. ^{1}H NMR (500 MHz, $CDCl_3$) δ: 8.07 (t, *J* = 7.9 Hz, 4H), 7.77 (t, *J* = 7.5 Hz, 2H), 7.63 (t, *J* = 7.8 Hz, 4H), 5.77 (dd, *J* = 10.8, 17.5 Hz, 1H), 5.09 (s, 4H), 5.04–4.82 (m, 5H), 4.73 (s, 5H), 3.73–3.61 (m, 4H), 3.34 (dd, *J* = 12.0, 30.2 Hz, 4H), 3.22–3.11 (m, 1H), 3.08–2.95 (m, 2H), 2.92–2.75 (m, 4H), 2.72–2.66 (m, 1H), 2.63–2.52 (m, 3H), 2.46 (t, *J* = 7.1 Hz, 8H), 2.32 (t, *J* = 7.2 Hz, 5H), 1.99 (dp, *J* = 6.3, 7.5, 22.2 Hz, 6H), 1.59 (dd, *J* = 9.0, 21.0 Hz, 2H), 1.52–1.38 (m, 4H), 0.96 (s, 3H); ^{13}C NMR (125 MHz, $CDCl_3$) *δ* 172.6, 170.3, 158.1, 150.0, 150.0, 149.4, 138.0, 135.9, 129.9, 128.8, 110.8, 110.7, 110.6, 110.5, 110.4, 110.2, 84.2, 78.6, 61.0, 60.2, 58.8, 53.6, 52.5, 51.9, 51.8, 51.3, 48.9, 48.5, 42.5, 42.5, 42.4, 41.2, 40.6, 40.0, 39.9, 33.6, 33.3, 29.8, 27.4, 20.1, 16.1. HR-ESI-MS *m/z* 1237.4587 (Calcd. for $C_{61}H_{72}N_8O_{16}S_2$ $[M + H]^+$, 1237.458).

Biological evaluation

NO release test

The Nanjing Jiancheng Biological Engineering Research Institute (A013-2-1) provided the kit to determine NO. The detailed procedure used to evaluate NO release was as documented in our earlier studies as well as in other referenced works [26, 27].

Anti-proliferative assay

Our study employed multiple cell lines K562, CCRF-CEM, A375, and SK-MEL-2, which were provided by Jiangsu Keygen Biotech Co., Ltd. We determined the anti-proliferative effects of our compounds using the CCK-8 cell proliferation assay. This assay is a standard method, the specifics of which were aligned with protocols previously detailed by our group and corroborated by other researchers [26].

K562 xenograft tumor mouse model

Experimental animals included female BALB/c nude mice (Shanghai Lingchang Biotechnology Co., Ltd.) weighing 19.0–20.0 g. The suspension of cultured K562 cells was collected at a concentration of 5×10^7 cell/mL. Each mouse was then subcutaneously injected with 0.1 mL of the suspension in the right axilla. When the diameter of the transplanted tumor reached 50–100 mm^3, the mice were divided into three groups, each comprising six mice. Two of these groups were then treated with *β*-elemene (30 $mg \cdot kg^{-1}$) and compound **13d** (30 $mg \cdot kg^{-1}$) for 28 days, respectively (i.v.). The model group was treated with the same amount of solvent. The tumor was excised from the mice and subsequently weighed.

References

[1] Radich J, Yeung C, Wu D. New approaches to molecular monitoring in CML (and other diseases) [J]. *Blood*, 2019, **134**(19): 1578-1584.

[2] Shono Y, van den Brink MRM. Gut microbiota injury in allogeneic haematopoietic stem cell transplantation [J]. *Nat Rev Cancer*, 2018, **18**(5): 283-295.

[3] Warraich Z, Tenneti P, Thai T, *et al*. Relapse prevention with tyrosine kinase inhibitors after allogeneic transplantation for philadelphia chromosome-positive acute lymphoblast leukemia: a systematic review [J]. *Biol Blood Marrow Tr*, 2020, **26**(3): e55-e64.

[4] Xu L, Tao S, Wang X, *et al*. The synthesis and anti-proliferative effects of *β*-elemene derivatives with mTOR inhibition activity [J]. *Bioorgan Med Chem*, 2006, **14**(15): 5351-5356.

[5] Garg N, Luzzatto-Knaan T, Melnik AV, *et al*. Natural products as mediators of disease [J]. *Nat Prod Rep*, 2017, **34**(2): 194-219.

[6] Bao R, Zhang H, Tang Y. Biomimetic synthesis of natural products: a journey to learn, to mimic, and to be better [J]. *Acc Chem Res*, 2021, **54**(19): 3720-3733.

[7] Zhang L, Song J, Kong L, *et al*. The strategies and techniques

of drug discovery from natural products [J]. *Pharmacol Therapeut*, 2020, **216**: 107686.
[8] Wang S, Dong G, Sheng C. Structural simplification of natural products [J]. *Chem Rev*, 2019, **119**(6): 4180-4220.
[9] Rodrigues T, Reker D, Schneider P, *et al*. Counting on natural products for drug design [J]. *Nat Chem*, 2016, **8**(6): 531-541.
[10] Harvey AL, Edrada-Ebel R, Quinn RJ. The re-emergence of natural products for drug discovery in the genomics era [J]. *Nat Rev Drug Discov*, 2015, **14**(2): 111-129.
[11] Azab A, Nassar A, Azab AN. Anti-inflammatory activity of natural products [J]. *Molecules*, 2016, **21**(10): 1321.
[12] Bai Z, Yao C, Zhu J, *et al*. Anti-tumor drug discovery based on natural product *β*-elemene: antitumor mechanisms and structural modification [J]. *Molecules*, 2021, **26**(6): 1499.
[13] He X, Zhuo XT, Gao Y, *et al*. *β*-Elemene derivatives produced from SeO_2-mediated oxidation reaction [J]. *R Soc Open Sci*, 2020, **7**(5): 200038.
[14] Lu JJ, Dang YY, Huang M, *et al*. Anti-cancer properties of terpenoids isolated from Rhizoma Curcumae–a review [J]. *J Ethnopharmacol*, 2012, **143**(2): 406-411.
[15] Zhai B, Zeng Y, Zeng Z, *et al*. Drug delivery systems for elemene, its main active ingredient *β*-elemene, and its derivatives in cancer therapy [J]. *Int J Nanomed*, 2018, **13**: 6279-6296.
[16] Chen J, Duan W, Bai R, *et al*. Design, synthesis and antioxidant activity evaluation of novel *β*-elemene derivatives [J]. *Bioorg Med Chem Lett*, 2014, **24**(15): 3407-3411.
[17] Huang Z, Fu J, Zhang Y. Nitric oxide donor-based cancer therapy: advances and prospects [J]. *J Med Chem*, 2017, **60**(18): 7617-7635.
[18] Farah C, Michel LYM, Balligand JL. Nitric oxide signalling in cardiovascular health and disease [J]. *Nat Rev Cardiol*, 2018, **15**(5): 292-316.
[19] Hibbs JB Jr, Taintor RR, Vavrin Z. Macrophage cytotoxicity: role for L-arginine deiminase and imino nitrogen oxidation to nitrite [J]. *Science*, 1987, **235**(4787): 473-476.
[20] Choudhari SK, Chaudhary C, Bagde S, *et al*. Nitric oxide and cancer: a review [J]. *World J Surg Oncol*, 2013, **11**: 118.
[21] Li Z, Xu X, Liu R, *et al*. Nitric oxide donor-based FFA1 agonists: design, synthesis and biological evaluation as potential antidiabetic and anti-thrombotic agents [J]. *Bioorgan Med Chem*, 2018, **26**(15): 4560-4566.
[22] Xie YD, Shao LH, Wang QT, *et al*. Design, synthesis and evaluation of phenylfuroxan nitric oxide-donor phenols as potential anti-diabetic agents [J]. *Bioorg Chem*, 2019, **89**: 103000.
[23] Halder AK, Mukherjee A, Adhikari N, *et al*. Nitric oxide synthase (NOS) inhibitors in cancer angiogenesis [J]. *Curr Enzym Inhib*, 2016, **12**(1): 49-66.
[24] Vivarelli S, Falzone L, Basile MS, *et al*. Nitric oxide in hematological cancers: partner or rival? [J]. *Antioxid Redox Sign*, 2021, **34**(5): 383-401.
[25] Kolb JP. Mechanisms involved in the pro- and anti-apoptotic role of NO in human leukemia [J]. *Leukemia*, 2000, **14**(9): 1685-1694.
[26] Chen J, Wang T, Xu S, *et al*. Discovery of novel antitumor nitric oxide-donating *β*-elemene hybrids through inhibiting the PI_3K/Akt pathway [J]. *Eur J Med Chem*, 2017, **135**: 414-423.
[27] Bai R, Zhu J, Bai Z, *et al*. Second generation *β*-elemene nitric oxide derivatives with reasonable linkers: potential hybrids against malignant brain glioma [J]. *J Enzym Inhib Med Ch*, 2022, **37**(1): 379-385.

Cite this article as: ZHU Junlong, JIANG Xiaoying, LUO Xinyu, GAO Yuan, ZHAO Rui, LI Junjie, CAI Hong, DANG Xiawen, YE Xiangyang, BAI Renren, XIE Tian. Discovery and bioassay of disubstituted *β*-elemene-NO donor conjugates: synergistic enhancement in the treatment of leukemia [J]. *Chin J Nat Med*, 2023, **21**(12): 916-926.